Chapter 7
Digital Band-pass Modulation Techniques

Problem 7.1
Invoking the band-pass assumption, show that

$$\int_0^{T_b} \sin(2\pi f_c t)\cos(2\pi f_c t)dt \approx 0$$

regardless of how the bit duration T_b is exactly related to f_c so long as $f_c >> 1/T_b$.

Solution
Let

$$I(T_b) = \int_0^{T_b} \sin(2\pi f_c t)\cos(2\pi f_c t)dt$$

Using the trigonometric identity

$$\sin(A)\cos(A) = \frac{1}{2}\sin(2A)$$

we may express $I(T_b)$ as

$$\begin{aligned}
I(T_b) &= \frac{1}{2}\int_0^{T_b} \sin(4\pi f_c t)dt \\
&= \frac{1}{2} \cdot \frac{1}{4\pi f_c}\cos(4\pi f_c t)\Big|_{t=0}^{T_b} \\
&= \frac{1}{8\pi f_c}[\cos(4\pi f_c T_b) - 1]
\end{aligned}$$

So long as $f_c > \frac{1}{T_b}$, we may set $\cos(4\pi f_c T_b) \approx 1$, in which case, $I(T_b) \approx 0$, thereby obtaining the desired result.

Problem 7.2
Show that Eq. (7.8) is *invariant* with respect to the carrier phase ϕ_c (i.e., it holds for all ϕ_c).

Solution
Assuming a carrier phase ϕ_c, the carrier is itself written as $\cos(2\pi f_c t + \phi_c)$. Then Eq. (7.7) modifies to

$$\begin{aligned}
E_b &= \int_0^{T_b} |s(t)|^2 dt \\
&= \frac{1}{T_b}\int_0^{T_b} |b(t)|^2 + \frac{1}{T_b}\int_0^{T_b} |b(t)|^2 \cos(4\pi f_c t + 2\phi_c)dt
\end{aligned}$$

where we have made use of the trigonometric identity

$$\cos^2\theta = \frac{1}{2}(\cos(2\theta))$$

Hence, with $|b(t)|^2$ remaining essentially constant over one complete cycle of $\cos(4\pi f_c t + 2\phi_c)$, we have

$$\int_0^{T_b} |b(t)|^2 \cos(4\pi f_c t + \phi_c) dt \approx 0 \text{ for all } \phi_c$$

Correspondingly, we may write

$$E_b = \int_0^{T_b} |b(t)|^2 \quad \text{for all } \phi_c.$$

Problem 7.3

Although QPSK and OQPSK signals have different waveforms, their magnitude spectra are identical; but their phase spectra differ by a nonlinear phase component. Justify the validity of this two-fold statement.

Solution

In QPSK, the modulated signal is defined by (see Eq. (7l15))

$$s_{\text{QPSK}}(t) = \sqrt{\frac{2E}{T}}\cos\left[(2i-1)\frac{\pi}{4}\right]\cos(2\pi f_c t) - \sqrt{\frac{2E}{T}}\sin\left[(2i-1)\frac{\pi}{4}\right]\sin(2\pi f_c t) \tag{1}$$

where $0 \le t \le T$ the index $i = 1,2,3,4$, depending on which particular dibit is sent. For a specific index i, the in-phase component of $S_{\text{QPSK}}(t)$ is therefore

$$s_{I,\,\text{QPSK}}(t) = \sqrt{\frac{2E}{T}}\cos\left[(2i-1)\frac{\pi}{4}\right], \qquad 0 \le t \le T \tag{2a}$$

and its quadrature component is

$$s_{Q,\,\text{QPSK}}(t) = \sqrt{\frac{2E}{T}}\sin\left[(2i-1)\frac{\pi}{4}\right], \qquad 0 \le t \le T \tag{2b}$$

In OQPSK, the in-phase component is left intact but the quadrature component is delayed by $T/2$ (half symbol period). Accordingly, for the same index i in QPSK, we may express the in-phase component of OQPSK as

$$s_{I,\,\text{OQPSK}}(t) = \sqrt{\frac{2E}{T}}\cos\left[(2i-1)\frac{\pi}{4}\right], \qquad 0 \le t \le T \tag{3a}$$

and its quadrature component as

$$s_{Q,\,\text{OQPSK}}(t) = \sqrt{\frac{2E}{T}}\sin\left[(2i-1)\frac{\pi}{4}\right], \qquad \frac{T}{2} \le t \le \frac{3}{2}T \tag{3b}$$

Let $b_I(t)$ denote a rectangular pulse of duration T, representing the in-phase component of the QPSK signal and $b_Q(t)$ denote the corresponding quadrature component. Then, in light of Eqs. (2) and (3), we may express the complex envelope of QPSK as

$$\tilde{s}_{\text{QPSK}}(t) = b_I(t) + jb_Q(t), \qquad 0 \le t \le T \tag{4}$$

and

$$\tilde{s}_{\text{OQPSK}}(t) = b_I(t) + jb_Q\left(t - \frac{T}{2}\right), \qquad 0 \le t \le T \tag{5}$$

Applying the Fourier transform to Eqs. (4) and (5), we correspondingly have

$$\tilde{s}_{\text{QPSK}}(f) = B_I(f) + jB_Q(f) \tag{6}$$

and

$$\begin{aligned}\tilde{s}_{\text{OQPSK}}(f) &= B_I(f) + jB_Q(f)\exp(-j\pi f\tau) \\ &= B_I(f) + jB_Q(f)[\cos(\pi f\tau) j\sin(\pi f\tau)] \\ &-[B_I(f)B_Q(f)\sin(\pi f\tau)] + jB_Q(f)\cos(\pi f\tau)\end{aligned} \tag{7}$$

From Eqs. (6) and (7), it therefore follows that for the QPSK

$$\left|\tilde{s}_{\text{QPSK}}(f)\right|^2 = B_I^2(f) + B_Q^2(f) \tag{8a}$$

and

$$\arg[\tilde{s}_{\text{QPSK}}(f)] = \tan^{-1}\left(\frac{B_Q(f)}{B_I(f)}\right) \tag{8b}$$

Similarly, for the OQPSK

$$\begin{aligned}\tilde{s}_{\text{OQPSK}}(f)\big|^2 &= [B_I(f)\ \text{-}\ B_Q\sin(\pi f\tau)]^2 + [B_Q(f)\cos(\pi fT)]^2 \\ &= B_I^2(f) + B_Q^2(f) - 2B_I(f)B_Q(f)\sin(\pi fT)\end{aligned} \tag{9a}$$

and

$$\arg[\tilde{s}_{\text{OQPSK}}(f)] = \tan^{-1}\left[\frac{B_Q(f)\cos(\pi fT)}{B_I(f) - B_Q\sin(\pi fT)}\right] \tag{9b}$$

For a square wave input, we typically find that the cross-product term $2B_I(f)B_Q(f)\sin(\pi fT)$ is small compared to the composite term $B_I^2(f) + B_Q^2(f)$. Accordingly, from Eqs. (8a) and (9a), it follows that for all practical purposes, the magnitude spectra $|S_{\text{QPSK}}(f)|$ and $|S_{\text{OQPSK}}(f)|$ are identical. In direct contrast, however, from Eqs. (8b) and (9b), we find that the corresponding phase spectra are not only different but the difference between them is a nonlinear function of frequency f.

Note: In the problem statement, the following correction should be made:
The term "linear phase component" is replaced by "nonlinear phase component".

Problem 7.4

Show that the modulation process involved in generating Sunde's BFSK is nonlinear.

Solution

Let

$$f_1 = f_c + \frac{1}{2T_b}, \quad \text{for symbol 1}$$

and

$$f_2 = f_c + \frac{1}{2T_b}, \quad \text{for symbol 0}$$

where f_c is the unmodulated carrier frequency. We may therefore express the instantaneous frequency of Sunde's BFSK signal as

$$f_i(t) = f_c + k\frac{1}{2T_b}, \qquad 0 \le t \le T_b \tag{1}$$

where

$$k = \begin{cases} +1 \text{ for symbol } 1 \\ -1 \text{ for symbol } 0 \end{cases}$$

Correspondingly, we may define the BFSK signal itself as

$$\begin{aligned} s(t) &= \sqrt{\frac{2E_b}{T_b}}\cos[2\pi f_i t] \\ &= \sqrt{\frac{2E_b}{T_b}}\cos\left(2\pi f_c t + \frac{\pi k}{T_b}t\right) \\ &= \sqrt{\frac{2E_b}{T_b}}\cos(2\pi f_c t)\cos\left(\frac{\pi k}{T_b}t\right) - \sqrt{\frac{2E_b}{T_b}}\sin(2\pi f_c t)\sin\left(\frac{\pi k}{T_b}t\right) \\ &= \sqrt{\frac{2E_b}{T_b}}\cos(2\pi f_c t)\cos\left(\pm\frac{\pi}{T_b}t\right) - \sqrt{\frac{2E_b}{T_b}}\sin(2\pi f_c t)\sin\left(\pm\frac{\pi}{T_b}t\right) \end{aligned} \tag{2}$$

Recognizing that

$$\cos(-A) = \cos A$$

and

$$\sin(-A) = -\sin A$$

we may rewrite Eq. (2) in the new form

$$s(t) = \sqrt{\frac{2E_b}{T_b}}\cos(2\pi f_c t)\cos\left(\frac{\pi}{T_b}t\right) \mp \sqrt{\frac{2E_b}{T_b}}\sin(2\pi f_c t)\sin\left(\frac{\pi}{T_b}t\right) \tag{3}$$

where $0 \le t \le T_b$; the minus sign corresponds to symbol 0 and the plus sign corresponds to symbol 1. Equation (3) reveals the following two characteristics of Sunde's BFSK:

(i) The in-phase component of $s(t)$ is independent of the incoming binary data stream.

(ii) The incoming binary data stream only affects the quadrature component.

It is because of property (ii) that we may go on to state that Sunde's BFSK is nonlinear.

Problem 7.5

To summarize matters, we may say that MSK is an OQPSK where the symbols in the in-phase and quadrature components (on a dibit-by-dibit basis) are weighted by the basic pulse function

$$p(t) = \sin\left(\frac{\pi t}{2T_b}\right)\text{rect}\left(\frac{t}{2T_b} - \frac{1}{2}\right)$$

where T_b is the bit duration, and rect(t) is the rectangular function of unit duration and unit amplitude. Justify this summary.

Solution

With $f_0 = \dfrac{1}{4T_b}$, it follows that

$$\cos(2\pi f_0 t) = \cos(\pi t/2T_b) = \sin\left[(\pi t/2T_b) + \frac{\pi}{2}\right] = \sin\left(\pi\left(\frac{t}{2T_b} + \frac{1}{2}\right)\right)$$

and

$$\sin(2\pi f_0 t) = \sin(\pi t/2T_b)$$

Following Eqs. (7.29) and (7.30), we next note that the binary waves $a_1(t)$ and $a_2(t)$, constituting the MSK signal, are extracted from the incoming binary data stream through demultiplexing and offsetting in a manner similar to OQPSK. Since $a_1(t)$ and $a_2(t)$ are themselves weighted by the sinusoidal functions $\cos(2\pi f_0 t)$ and $\sin(2\pi f_0 t)$, we may go on to state that the in-phase and quadrature components of the MSK signal are weighted (on a dibit-by-dibit basis) by the basic pulse function

$$p(t) = \sin\left(\frac{\pi t}{2T_b}\right)\text{rect}\left(\frac{t}{2T_b} - \frac{1}{2}\right)$$

Problem 7.6

The sequence 11011100 is applied to an MSK modulator. Assuming that the angle $\theta(t)$ of the MSK signal is zero at time $t = 0$, plot the trellis diagram that displays the evolution of $\theta(t)$ over the eight binary symbols of the input sequence.

Solution

Evolution of the phase $\theta(t)$ of the MSK signal produced by the sequence 11011100 is displayed in Fig. 1.

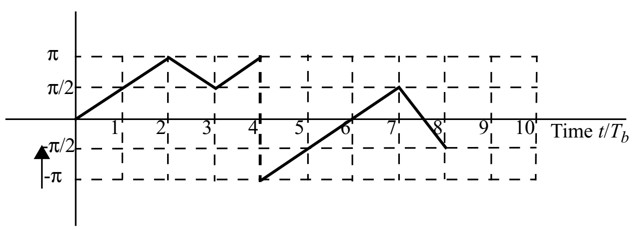

Figure 1

Problem 7.7

The process of angle modulation involved in the generation of an MSK signal is linear. Justify this assertion.

Solution

We first recognize from Problem 7.5 that MSK is an OQPSK signal with only a basic difference:

(i) In OQPSK, the weighting applied to the in-phase and quadrature components of the modulated signal (on a dibit-by-dibit basis) is in the form of a rectangular function. On the other hand, in MSK, the corresponding weighting functions are sinusoidal.

(ii) The OQPSK is the result of a linear modulation process.

In light of these two points, we may therefore state that the angle modulation process involved in generating MSK is a linear process.

Problem 7.8
A simple way of demodulating an MSK signal is to use a frequency discriminator, which was discussed in Chapter 4 on angle modulation. Justify this use and specify the linear input-output characteristic of the discriminator.

Solution
The MSK signal is basically an FSK signal, as shown by

$$s(t) = \sqrt{\frac{2E_b}{T_b}}\cos(2\pi f_c t + \theta(t))$$

where

$$\theta(t) = \pm\frac{\pi t}{2T_b}$$

The plus sign corresponds to symbol 1 and the minus sign corresponds to symbol 0.

We may therefore demodulate $s(t)$ by using a frequency discriminator whose input-output characteristic is described in Fig. 1

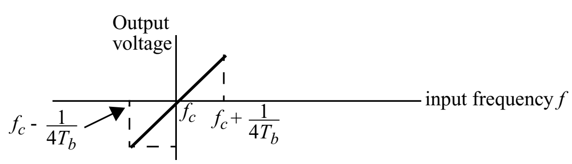

Figure 1

Problem 7.9
Starting with Eq. (7.41), prove the orthogonality property of Eq. (7.42) that characterizes M-ary FSK.

Solution
From Eq. (7.41), we have

$$s_i(t) = \sqrt{\frac{2E}{T}}\cos\left[\frac{\pi}{T}(n+i)t\right] \qquad \begin{array}{l} i = 0, 1, \ldots, M\text{-}1 \\ 0 \le t \le T \end{array}$$

Applying Eq. (7.42), we therefore have

$$\int_0^T s_i(t)s_j(t)dt = \frac{2E}{T}\int_0^T \cos\left[\frac{\pi}{T}(n+i)t\right]\cos\left[\frac{\pi}{T}(n+j)t\right]dt$$

$$= \frac{E}{T}\int_0^T \left\{\cos\left[\frac{\pi}{T}(2n+i+j)t\right] + \cos\left[\frac{\pi}{T}(i-j)t\right]\right\}dt \qquad (1)$$

Let the integer $k = 2n + i + j$, and $i - j = l$ for $i \neq j$. We may then rewrite Eq. (1) as

$$\int_0^T s_i(t)s_j(t)dt = \frac{E}{T}\int_0^T \left\{\cos\left(\frac{\pi}{T}kt\right) + \cos\left(\frac{\pi}{T}lt\right)\right\}dt$$

$$= \frac{E}{T}\left[\frac{T}{k\pi}\sin\left(\frac{\pi}{T}kt\right) + \frac{T}{l\pi}\sin\left(\frac{\pi}{T}lt\right)\right]_{t=0}^{T}$$

$$= \; 0 \;\text{ for all integer } k \text{ and } l$$

which is the desired result.

Problem 7.10

Justify Eqs. (7.47) and (7.49).

Solution

Starting with Eq. (7.47), we write

$$\mathbf{s}_1 \;=\; \frac{2}{T_b}\sqrt{E_b}\;\int_0^{T_b}\cos^2(2\pi f_c t)dt$$

$$= \;\frac{1}{T_b}\sqrt{E_b}\int_0^{T_b}[\cos^2(4\pi f_c t) + 1]dt \qquad (1)$$

For $f_c = n/T_b$ for some integer n, Eq. (1) takes the form

$$\mathbf{s}_1 \;=\; \frac{\sqrt{E_b}}{T_b}\;\int_0^{T_b}\left[\cos\left(\frac{4\pi n}{T_b}t\right) + 1\right]dt$$

$$= \;\frac{\sqrt{E_b}}{T_b}\left[\frac{T_b}{4\pi n}\sin\left(\frac{4\pi n}{T_b}t\right) + t\right]_0^{T_b}$$

$$= \;\frac{\sqrt{E_b}}{T_b}\left[\frac{T_b}{4\pi n}\sin(4\pi n) + T_b\right], \quad n \text{ integer}$$

$$= \;\sqrt{E_b}$$

Similarly, for symbol 0, we have

$$\mathbf{s}_2 \;=\; -\sqrt{E_b}$$

Problem 7.11

(a) The transmission bandwidth of the BASK signal is effectively defined by

$$B_T \;=\; \frac{2}{T_b}$$

where T_b is the bit duration. With $T_b = 1\,\mu\text{s}$, we therefore have

$$B_T \;=\; \frac{2}{10^{-6}}\;\text{ Hz}$$

$$= \;2\;\text{ MHz}$$

(b)

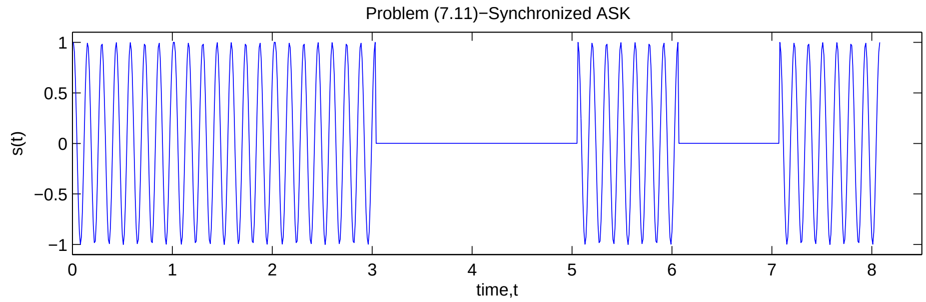

Figure 1

In the waveform plotted in Fig. 1, time t is measured in microseconds.

Problem 7.12

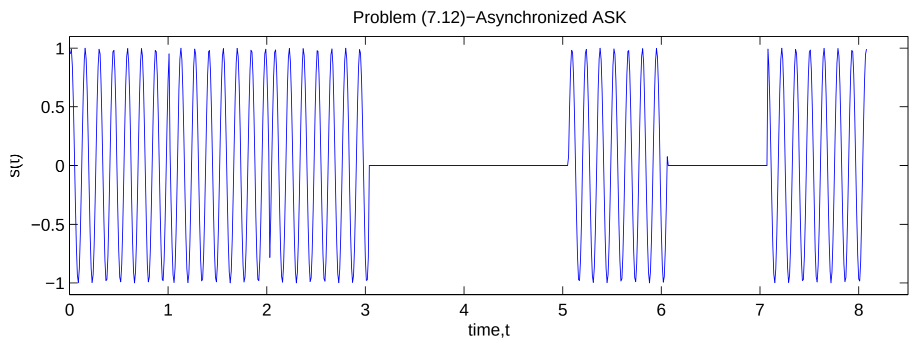

Figure 1, where time t is measured in microseconds

Comparing the BASK waveform plotted in Fig. 1 of this solution with that of the BASK signal considered in Problem 7.11, we see that continuity in time is not maintained in Fig. 1 of the solution to Problem 7.12, when a succession of 1s is transmitted.

Problem 7.13

(a)

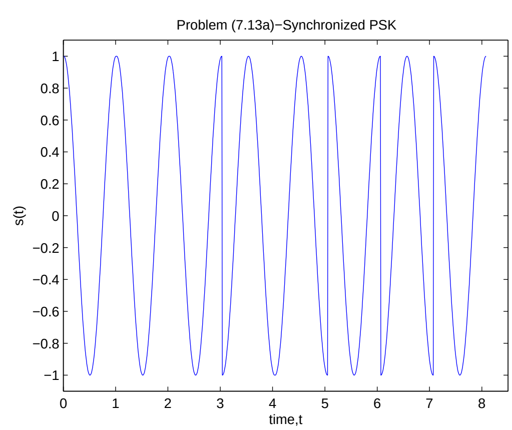

Figure 1

(b)

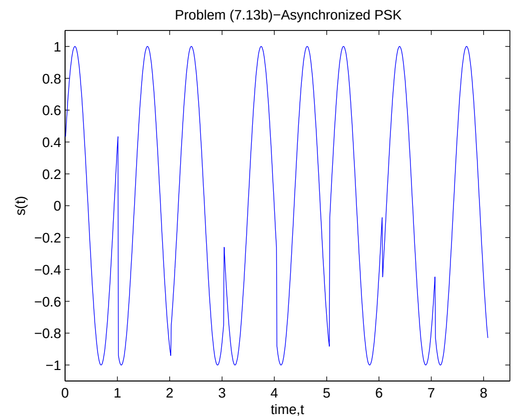

Figure 2

<u>Notes</u>:

(i) In both Figures 1 and 2, time t is measured in microseconds.

(ii) For clarity of presentation, the carrier frequency in both figures has been scaled down from 7 MHZ to 1 MHZ.

(iii) In Fig. 1 of the solution, there is synchronism between the carrier phase and the times at which the incoming data switch for symbol 1 or 0 or vice versa. No such synchronism exists in Fig. 2.

Problem 7.14

(a) The transmission bandwidth of the QPSK signal is

$$B_T = \frac{2}{T} = \frac{2}{2T_b} = \frac{1}{T_b}$$

where T is the symbol (dibit) duration and T_b is the bit duration. With $T_b = 1\mu s$, it follows therefore that

$$B_T = \frac{1}{10^{-6}} \text{ Hz}$$
$$= 1 \text{ MHz}$$

(b)

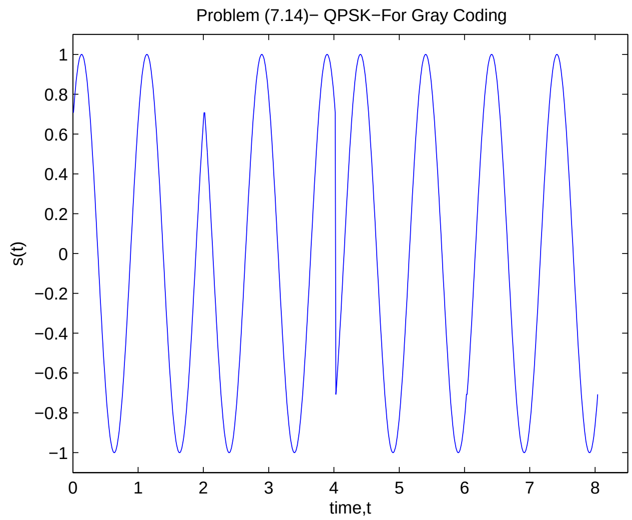

Figure 1

<u>Notes</u>:

(i) Time t in Fig. 1 is measured in microseconds.

(ii) For clarify of presentation, we have plotted the QPSK waveform using a carrier of 1 MHz instead of 6 MHz.

(iii) Synchronism between the timing waveform representing the incoming binary data stream and the clock responsible for generating the carrier is assumed.

Problem 7.15

(a) The transmission bandwidth of OQPSK is exactly the same as that of QPSK, which, for the problem at hand, is 1 MHz.

(b)

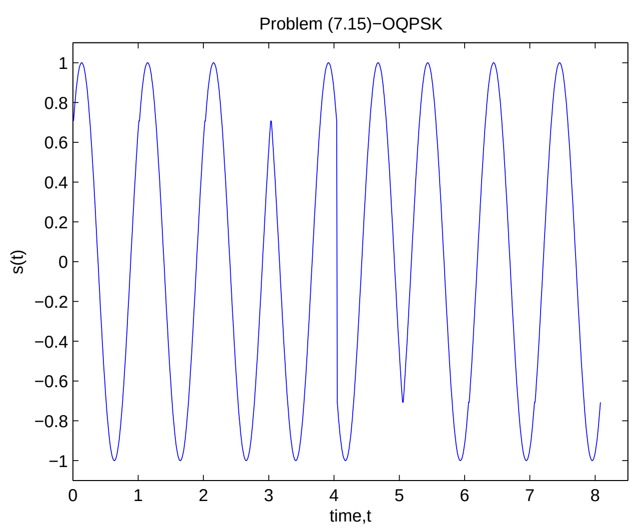

Figure 1

In plotting the OQPSK waveform in Fig. 1, we have followed the same notes made in the solution to Problem 7.14 on QPSK.

Problem 7.16

(a) The transmission bandwidth of Sunde's BFSK is greater than that of the corresponding BPSK. This means that for the problem at hand, it will be greater than 1 MHz. In particular, examining the spectrum shown in Fig. 7.12, we see that the main lobe occupies a bandwidth of 3 Hz for the bit duration $T_b = 1$s. Therefore, scaling this result for $T_b = 1\mu$s, we may say that the corresponding transmission bandwidth is

$$B_T = 3 \text{ MHz}$$

which is 50% greater than that of the corresponding BPSK.

(b)

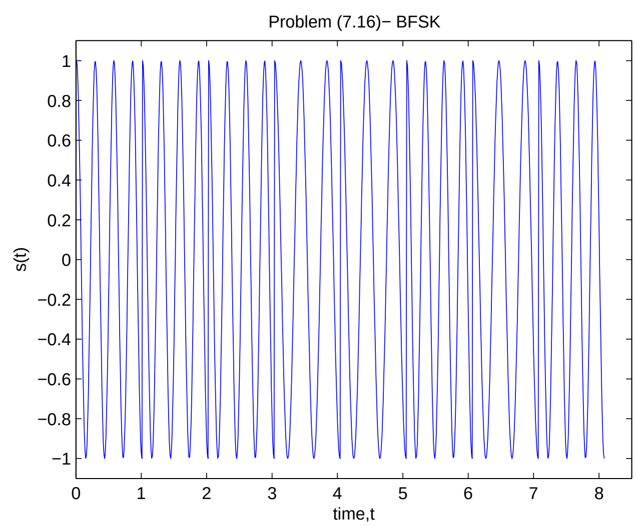

Figure 1

Notes:

In plotting the BFSK waveform in Fig. 1, we have followed the same notes outlined in the solution to Problem 7.14.

Problem 7.17

(a) Examining the continuous phase FSK waveform plotted in Fig. 7.1(c), we observe the following two points (assuming that time t is measured in seconds):

(i) The carrier for symbol 00 occupies 3 complete cycles. Therefore,

$$f_2 = \frac{1}{(2 \text{ seconds})/(3 \text{ cycles})} = 1.5 \text{ Hz}$$

(ii) The carrier for symbol 11 occupies 5 complete cycles. Therefore,

$$f_1 = \frac{1}{(2 \text{ seconds})/(5 \text{ cycles})} = 2.5 \text{ Hz}$$

Hence, the frequency excursion is

$$\delta f = f_1 - f_2$$
$$= 2.5 - 1.5 = 1 \ \text{Hz}$$

(b) The frequency parameter f_0 is defined by (see Eq. (7.34))

$$f_0 = \frac{1}{4T_b}$$
$$= \frac{1}{4 \times 1 \ \mu\text{s}} = 0.25 \ \text{MHz}$$

Problem 7.18

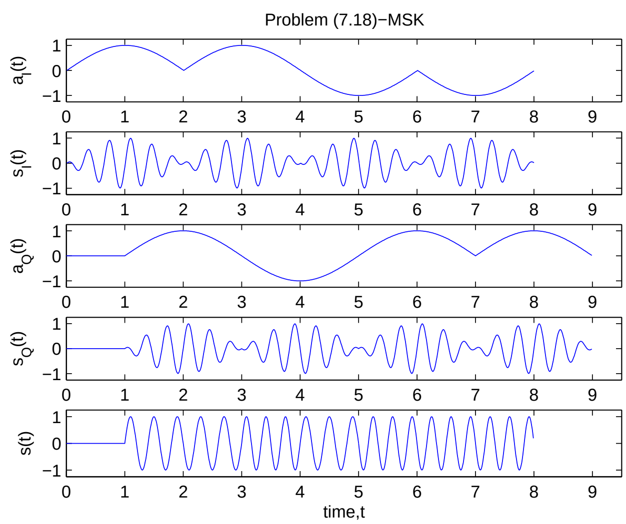

Figure 1

In plotting the MSK waveform and its constituents shown in Fig. 1, the following two points should be noted:

(i) Time t is measured in microseconds.

(ii) Synchronism is assumed between the timing waveform responsible for generating the incoming binary sequences (and therefore the constituent sequences $s_I(t)$ and $s_Q(t)$) and the clock responsible for generating the carrier.

Problem 7.19

The bit duration is

$$T_b = \frac{1}{20 \times 10^3} \ \text{seconds}$$
$$= 50 \ \mu\text{s}$$

The carrier frequency is

$$f_c = 50 \ \text{MHz}$$

From Eq. (7.19), the frequency excursion is

$$\delta f = \frac{1}{2T_b}$$

$$= \frac{1}{2 \times 50 \times 10^{-6}} \text{ Hz} = 10 \text{ kHz}$$

From Eqs. (7.21) and (7.22), we have

$$f_1 = f_c + \frac{\delta f}{2}$$

$$= 50 \text{ MHz} + 5 \text{ kHz}$$

$$= 50.005 \text{ MHz}$$

$$f_2 = f_c - \frac{\delta f}{2}$$

$$= 50 \text{ MHz} - 5 \text{ kHz}$$

$$= 49.995 \text{ MHz}$$

(a) The instantaneous frequency of the MSK signal is therefore

$$f_i(t) = \begin{cases} 50.005 \text{ MHz} & \text{for symbol 1} \\ 49.995 \text{ MHz} & \text{for symbol 0} \end{cases}$$

Specifically, $f_i(t)$ alternates between these two values.

(b) When the incoming data sequence consists of all 1s, we have

$f_i(t) = 50.005$ MHz for all time t

Problem 7.20

Extraction of the bit-timing may proceed as follows:

(i) Given the MSK signal $s(t)$, a band-pass analyzer is used to extract the in-phase component $s_I(t)$ and quadrature component $s_Q(t)$.

(ii) From the first line of Eq. (7.31), and Eqs. (7.33) and (7.34), we have

$$r(t) = \frac{s_Q(t)}{s_I(t)} = -\tan\left(\frac{\pi t}{2T_b}\right) = -\tan(\theta(t))$$

which depends on the bit duration T_b alone.

(iii) From Eq. (7.32), we recall that whenever two successive binary symbols in the original data stream are the same, then $\theta(t)$ is negative and therefore the ratio $r(t)$ is positive. On the other hand, from Eq. (7.33), we recall that whenever two successive binary symbols are different, then $\theta(t)$ is positive and therefore the ratio $r(t)$ is negative.

Hence, by observing the zero-crossings of the waveform obtained from $r(t) = [s_Q(t)/s_I(t)]$, it should be possible to extract the timing waveform.

Problem 7.21

The envelope of BFSK is constant with time, whereas the envelope of BASK is variable. Accordingly, the noncoherent receiver of Fig. 7.18 for BFSK offers the following practical advantages over the noncoherent receiver of Fig. 7.17 for BASK:
(i) Reduced sensitivity to nonlinear transmission.
(ii) Improved performance in the presence of channel noise and interference.

Problem 7.22

For the noncoherent receiver of Fig. 7.29 to offer an identical performance to the noncoherent receiver of Fig. 7.18, the following conditions must be satisfied:

(i) The bit-timing circuitry of both receivers must be equally accurate.
(ii) The common bandwidth of the band-pass filter must occupy at the minimum the main spectral lobe of the incoming BFSK signal. As such, a reasonably good choice for this bandwidth is the reciprocal of $2T_b$, where T_b is the bit duration.
(iii) With one band-pass filtered centred on f_1 and the other centred on f_2, the frequencies f_1 and f_2 must be separated from each other by at least $1/(2T_b)$.

These three conditions do not guarantee the exact equivalence of the two noncoherent receivers of Figs. 7.18 and 7.19, but, for all practical purposes, would assure identical performance.

Problem 7.23

(a) The transmission bandwidth of DSK signal is the same as that of the corresponding BPSK. Therefore, for a bit duration $T_b = 1\mu$s, the bandwidth is

$$B_T = \frac{2}{T_b} = 2 \times 10^{+6} \text{ Hz} = 2 \text{ MHz}$$

(b) In plotting the DPSK waveform shown in Fig. 1, we have followed three points:
   (i) Time t is measured in microseconds.
   (ii) For clarity of presentation, a carrier frequency $f_c = 1$ MHz has been used in place of $f_c = 6$ MHz.
   (iii) Synchronism is assumed between the timing circuitry responsible for line encoding the incoming binary data stream and the clock responsible for generating the carrier.

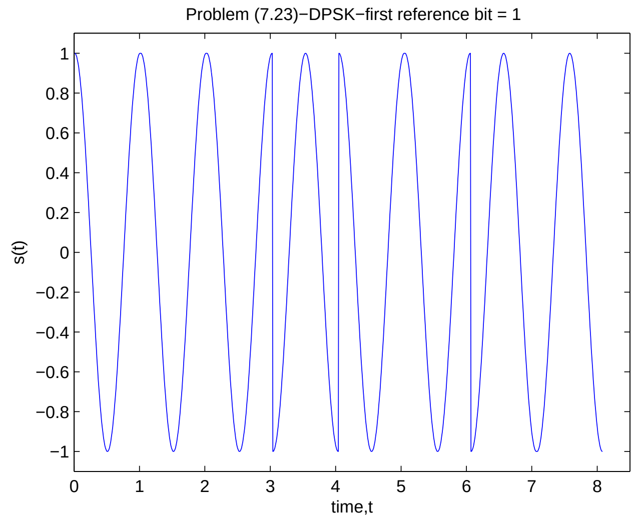

Figure 1

(c) Decoding in the receiver is first accomplished by multiplying the received signal by $\cos(2\pi f_c t)$ and then low-pass filtering. Next, the low-pass filter output is applied to a DPSK decoder. Thus, starting with a reference bit 1 and assuming perfect transmission (i.e., zero channel noise), the receiver output is the same as the original binary sequence, namely, 11100101.

Problem 7.24

(a) The noiseless PSK signal is given by

$$\begin{aligned} s(t) &= A_c \cos[2\pi f_c t + k_p m(t)] \\ &= A_c \cos(2\pi f_c t)\cos[k_p m(t)] - A_c \sin(2\pi f_c t)\sin[k_p m(t)] \end{aligned}$$

Since $m(t) = \pm 1$, it follows that

$$\cos[k_p m(t)] = \cos(\pm k_p) = \cos(k_p)$$

$$\sin[k_p m(t)] = \sin(\pm k_p) = \pm\sin(k_p) = m(t)\sin(k_p)$$

Therefore,

$$s(t) = A_c \cos(k_p)\cos(2\pi f_c t) - A_c m(t)\sin(k_p)\sin(2\pi f_c t) \tag{1}$$

The VCO output is

$$r(t) = A_v \sin[2\pi f_c t + \theta(t)]$$

The multiplier output in the phase-locked loop is therefore

$$\begin{aligned} r(t)s(t) = {} & \frac{1}{2}A_c A_v \cos(k_p)\{\sin[\theta(t)] + \sin[4\pi f_c t + \theta(t)]\} \\ & - \frac{1}{2}A_c A_v m(t)\sin(k_p)\{\cos(\theta(t)) + \cos[4\pi f_c t + \theta(t)]\} \end{aligned}$$

The loop filter removes the double-frequency components, producing the output

$$e(t) = \frac{1}{2}A_c A_v \cos(k_p)\sin[\theta(t)] - \frac{1}{2}A_c A_v m(t)\sin(k_p)\cos[\theta(t)]$$

Note that if $k_p = \pi/2$, (i.e., the carrier is fully deviated), there would be no carrier component for the PLL to track.

(b) Since the error signal tends to drive the loop into lock (i.e., $\theta(t)$ approaches zero), the loop filter output reduces to

$$e(t) = -\frac{1}{2}A_c A_v \sin(k_p) m(t)$$

which is proportional to the desired data signal $m(t)$. Hence, the phase-locked loop may be used to recover the original message $m(t)$.

Problem 7.25

(a) The correlation coefficient of the signals $s_0(t)$ and $s_1(t)$ is

$$\rho = \frac{\int_0^{T_b} s_0(t)s_1(t)dt}{\left[\int_0^{T_b} s_0^2(t)dt\right]^{1/2}\left[\int_0^{T_b} s_1^2(t)dt\right]^{1/2}}$$

$$= \frac{A_c^2\int_0^{T_b} \cos\left[2\pi\left(f_c + \frac{1}{2}\Delta f\right)t\right]\cos\left[2\pi\left(f_c - \frac{1}{2}\Delta f\right)t\right]}{\left[\frac{1}{2}A_c^2 T_b\right]^{1/2}\left[\frac{1}{2}A_c^2 T_b\right]^{1/2}}$$

$$= \frac{1}{T_b}\int_0^{T_b}[\cos(2\pi\Delta f t) + \cos(4\pi f_c t)]dt$$

$$= \frac{1}{2\pi T_b}\left[\frac{\sin(2\pi\Delta f T_b)}{\Delta f} + \frac{\sin(4\pi f_c T_b)}{2f_c}\right] \qquad (1)$$

Since $f_c >> \Delta f$, then we may ignore the second term in Eq. (1), obtaining

$$\rho \approx \frac{\sin(2\pi\Delta f T_b)}{2\pi T_b \Delta f} = \mathrm{sinc}(2\Delta f T_b)$$

(b) The dependence of ρ on Δf is as shown in Fig. 1. The two signals $s_0(t)$ and $s_1(t)$ are orthogonal when $\rho = 0$. Therefore, the minimum value of Δf for which they are orthogonal is $1/2T_b$.
$s_0(t)$ and $s_1(t)$ are orthogonal when $\rho = 0$. Therefore, the minimum value of Δf for which they are orthogonal is $1/2T_b$.

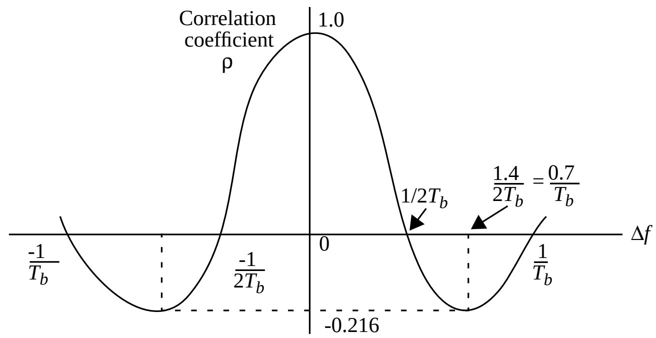

Figure 1

Problem 7.26

(a) The given binary FSK signal is defined by

$$s_{\text{FSK}}(t) = \begin{cases} \sqrt{\dfrac{2E_b}{T_b}}\cos(2\pi f_1 t + \theta_1) & \text{for symbol } 0 \\ \sqrt{\dfrac{2E_b}{T_b}}\cos(2\pi f_2 t + \theta_2) & \text{for symbol } 1 \end{cases} \tag{1}$$

Equation (1) may be expressed in the equivalent form

$$s_{\text{FSK}}(t) = s_1(t) + s_2(t) \tag{2}$$

where

$$s_1(t) = \begin{cases} \sqrt{\dfrac{2E_b}{T_b}}\cos(2\pi f_1 t + \theta_1) & \text{for symbol } 0 \\ 0 & \text{for symbol } 1 \end{cases} \tag{3}$$

and

$$s_2(t) = \begin{cases} 0 & \text{for symbol } 0 \\ \sqrt{\dfrac{2E_b}{T_b}}\cos(2\pi f_2 t + \theta_2) & \text{for symbol } 1 \end{cases} \tag{4}$$

The digitally modulated signals $s_1(t)$ and $s_2(t)$ are recognized as two complementary BASK signals, operating in parallel. In light of Eqs. (1) through (4), we may construct the two-transmitter equivalence depicted in Fig. 1.

(a)

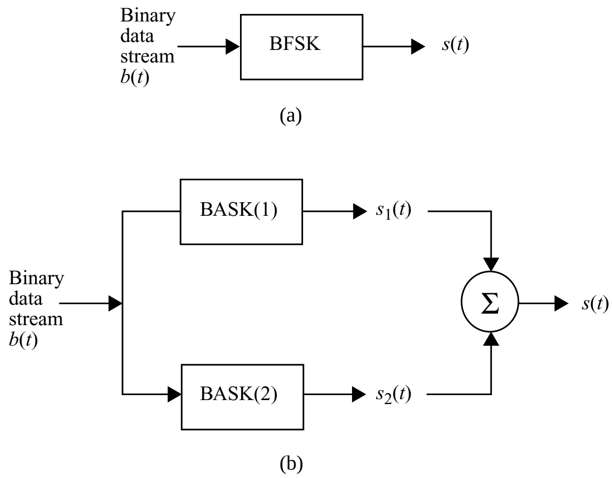

Figure 1

(b)

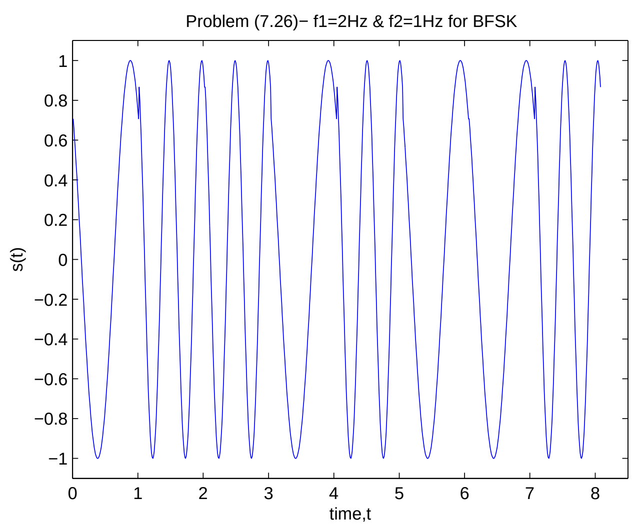

Problem 7.27

From the description of minimum-shift keying presented in Section 7.4, we recall the following:

- The transmission of symbol 1 increases the phase of the MSK signal by $\pi/2$ radians.
- The transmission of symbol 0 decreases the phase of the MSK signal by $\pi/2$ radians.

Accordingly, we may justify the entries listed in Table 7.4 as follows:

(a) When $\theta(0) = 0$, the transmission of symbol 0 yields

$$\theta(T_b) = -\pi/2 \quad \text{radians}$$

(b) When $\theta(0) = \pi$ radians, the transmission of symbol 1 yields

$$\theta(T_b) = \pi + \pi/2 = 3\pi/2 \quad \text{radians}$$

which, in modulo-2π arithmetic, is equivalent to

$\theta(T_b) = 3\pi/2 - 2\pi = -\pi/2$ radians

(c) When $\theta(0) = \pi$ radians, the transmission of symbol 0 yields

$\theta(T_b) = \pi - (\pi/2) = +\pi/2$ radians

(d) When $\theta(0) = 0$, the transmission of symbol 1 yields

$\theta(T_b) = 0 + \pi/2 = +\pi/2$ radians

Problem 7.28

The idea of quadrature multiplexing rests on the following premise: Two signals can be transmitted over a common channel, provided that two conditions are satisfied:

(i) The two signals are orthogonal to each other.

(ii) They both occupy the same bandwidth.

This principle is satisfied by quadriphase-shift keying (QPSK), as demonstrated next.

Consider the QPSK signal defined by

$$s(t) = \begin{cases} \sqrt{\dfrac{2E}{T}}\cos(2\pi f_c t), & \text{dibit } 00 \\ -\sqrt{\dfrac{2E}{T}}\sin((2\pi f_c t),) & \text{dibit } 01 \\ \sqrt{\dfrac{2E}{T}}\cos(2\pi f_c t + \pi), & \text{dibit } 11 \\ -\sqrt{\dfrac{2E}{T}}\cos(2\pi f_c t + \pi), & \text{dibit } 10 \end{cases} \tag{1}$$

This signal can be decomposed into the sum of two BPSK signals, defined as follows:

$$s_1(t) = \begin{cases} \sqrt{\dfrac{2E}{T}}\cos(2\pi f_c t), & \text{dibit } 00 \\ \sqrt{\dfrac{2E}{T}}\cos(2\pi f_c t + \pi), & \text{dibit } 11 \end{cases} \tag{2}$$

and

$$s_2(t) = \begin{cases} -\sqrt{\dfrac{2E}{T}}\sin(2\pi f_c t), & \text{dibit } 01 \\ -\sqrt{\dfrac{2E}{T}}\sin(2\pi f_c t + \pi), & \text{dibit } 10 \end{cases} \tag{3}$$

In light of Eqs. (1) through (3), we may write

$$s(t) = s_1(t) + s_2(t) \tag{4}$$

which means that $s_1(t)$ and $s_2(t)$ can be transmitted simultaneously on a common channel and be detected separately at the receiver. This statement is justified on two accounts:

(i) Both $s_1(t)$ and $s_2(t)$ occupy exactly the same bandwidth, as their magnitude spectra are identical.

(ii) They are orthogonal over the symbol period T, as shown by

$$\int_0^T s_1(t)s_2(t) = \int_0^T \sqrt{\frac{2E}{T}}\cos(2\pi f_c t)\left(-\sqrt{\frac{2E}{T}}\right)\sin(2\pi f_c t)dt$$

$$= -\frac{E}{T}\int_0^T \sin 4(\pi f_c t)dt$$

which is zero by the band-pass assumption, provided that the carrier frequency f_c is high enough.

The assertion embodied in Eq. (4) holds for any clockwise or counterclockwise rotation of the QPSK constellation defined in Eq. (1).

Consider next the 8-PSK defined by

$$s'(t) = \begin{cases} \sqrt{\frac{2E}{T}}\cos(2\pi f_c t), & \text{symbol } 000 \\ \sqrt{\frac{2E}{T}}\cos\left(2\pi f_c t + \frac{\pi}{4}\right), & \text{symbol } 001 \\ \sqrt{\frac{2E}{T}}\cos\left(2\pi f_c t + \frac{\pi}{2}\right), & \text{symbol } 101 \\ \sqrt{\frac{2E}{T}}\cos\left(2\pi f_c t + \frac{3\pi}{4}\right), & \text{symbol } 111 \\ \sqrt{\frac{2E}{T}}\cos(2\pi f_c t + \pi), & \text{symbol } 011 \\ \sqrt{\frac{2E}{T}}\cos\left(2\pi f_c t + \frac{5\pi}{4}\right), & \text{symbol } 010 \\ \sqrt{\frac{2E}{T}}\cos\left(2\pi f_c t + \frac{3\pi}{2}\right), & \text{symbol } 110 \\ \sqrt{\frac{2E}{T}}\cos\left(2\pi f_c t + \frac{7\pi}{4}\right), & \text{symbol } 100 \end{cases} \quad (5)$$

Following what we did with the QPSK signal of Eq. (1), we may decompose the 8-PSK of Eq. (5) as follows:

$s(t) = s'_1(t) + s'_2(t)$

whose constituents are defined by

$$s'_1(t) = \begin{cases} \sqrt{\frac{2E}{T}}\cos(2\pi f_c t), & \text{symbol } 000 \\ \sqrt{\frac{2E}{T}}\cos\left(2\pi f_c t + \frac{\pi}{2}\right), & \text{symbol } 101 \\ \sqrt{\frac{2E}{T}}\cos(2\pi f_c t + \pi), & \text{symbol } 011 \\ \sqrt{\frac{2E}{T}}\cos\left(2\pi f_c t + \frac{3\pi}{2}\right), & \text{symbol } 110 \end{cases} \tag{6}$$

and

$$s'_2(t) = \begin{cases} \sqrt{\frac{2E}{T}}\cos\left(2\pi f_c t + \frac{\pi}{4}\right), & \text{symbol } 001 \\ \sqrt{\frac{2E}{T}}\cos\left(2\pi f_c t + \frac{3\pi}{4}\right), & \text{symbol } 111 \\ \sqrt{\frac{2E}{T}}\cos\left(2\pi f_c t + \frac{5\pi}{4}\right), & \text{symbol } 010 \\ \sqrt{\frac{2E}{T}}\cos\left(2\pi f_c t + \frac{7\pi}{4}\right), & \text{symbol } 100 \end{cases} \tag{7}$$

Basically, the signal $s'_1(t)$ is a rewrite of the QPSK signal $s(t)$ of Eq. (1). The signal $s'_2(t)$ is a rotated version of $s(t)$. The two constituent QPSK signals $s'_1(t)$ and $s'_2(t)$ satisfy the common bandwidth requirement (i). However, they fail to satisfy requirement (ii). To demonstrate this failure, let us test the first components of $s'_1(t)$ and $s'_2(t)$ for orthogonality by writing

$$\begin{aligned} \int_0^T s'_1(t)s'_2(t) &= \int_0^T \sqrt{\frac{2E}{T}}\cos(2\pi f_c t) \cdot \sqrt{\frac{2E}{T}}\cos\left(2\pi f_c t + \frac{\pi}{4}\right)dt \\ &= \frac{2E}{T}\int_0^T \cos(2\pi f_c t)\cos\left(2\pi f_c t + \frac{\pi}{4}\right)dt \\ &= \frac{E}{T}\int_0^T \left[\cos\left(\frac{\pi}{4}\right) + \cos\left(4\pi f_c t + \frac{\pi}{4}\right)\right]dt \\ &= \frac{E}{T} \cdot \frac{T}{\sqrt{2}} + \frac{E}{T}\int_0^T \cos\left(4\pi f_c t + \frac{\pi}{4}\right)dt \end{aligned} \tag{8}$$

The integral term of Eq. (8) may be set equal to zero under the band-pass assumption, provided that the carrier frequency f_c is high enough. But the first term, namely, $E/\sqrt{2}$ is nonzero. We therefore conclude that the orthogonality requirement is violated by the two QPSK signals $s'_1(t)$

and $s'_2(t)$. Hence, The "conquer and divide" approach theorem cannot be exploited beyond the QPSK signal.

Problem 7.29

To simplify the presentation, hereafter we concentrate on the complex envelope (i.e., complex baseband signal) of the QPSK signal, and likewise for the OQPSK signal. Otherwise, the phase spectra of the QPSK and OQPSK signals would become dominated by the contribution of the carrier, which complicates the graphical plots.

Figure 1 plots the phase spectrum of the QPSK signal with a square wave applied to each of the *I*- and *Q*-channels. The phase spectrum has impulses spaced uniformly at the symbol rate, corresponding to the phase discontinuities that occur at the symbol rate.

Figure 2 plots the phase spectrum of the corresponding OQPSK spectrum, with the same square wave applied to each of the *I*- and *Q*-channels. The phase spectrum of Fig. 2 is similar to that of Fig. 1 for the QPSK in that both of them consist of a series of impulses. However, in Fig. 2 the impulses are shifted in frequency as well as amplitude. Moreover, the impulses in Fig. 2 are spaced by twice the symbol rate, because every second harmonic is cancelled out.

The phase spectra plotted in figs. 1 and 2 depend on the symbol rate of the incoming square wave and the way in which the square wave is positioned with respect to the origin (i.e., time $t = 0$).

Finally, Fig. 3 plots the phase difference between the QPSK and OQPSK. From this figure we readily see that this phase difference is a nonlinear function of frequency.

<u>Note</u>

The last sentence in the statement of Problem 7.29 should be corrected as follows:

"Hence, justify the assertion made in Drill Problem 7.3 that these two methods differ by a nonlinear phase component."

Also, add the following:

Hint: Use the complex envelope for the representation of QPSK and OQPSK signals.

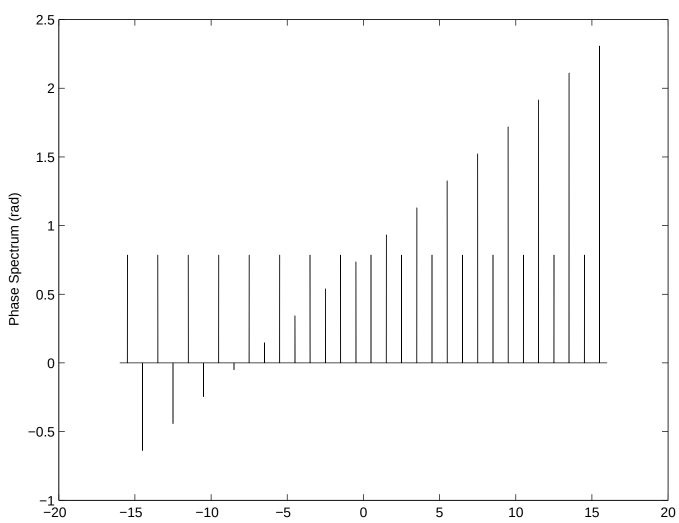

Phase spectrum of QPSK with square wave in each of *I* and *Q*-channels

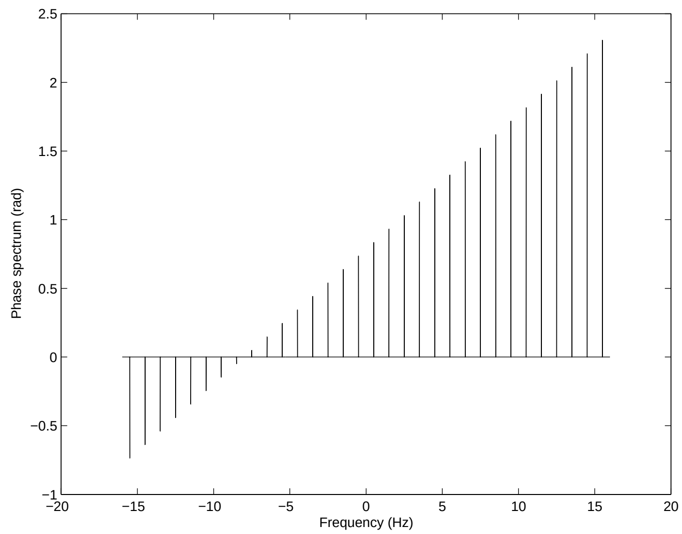

Figure 1

Phase spectrum of OQPSK with square wave in each of *I* and *Q*-channels

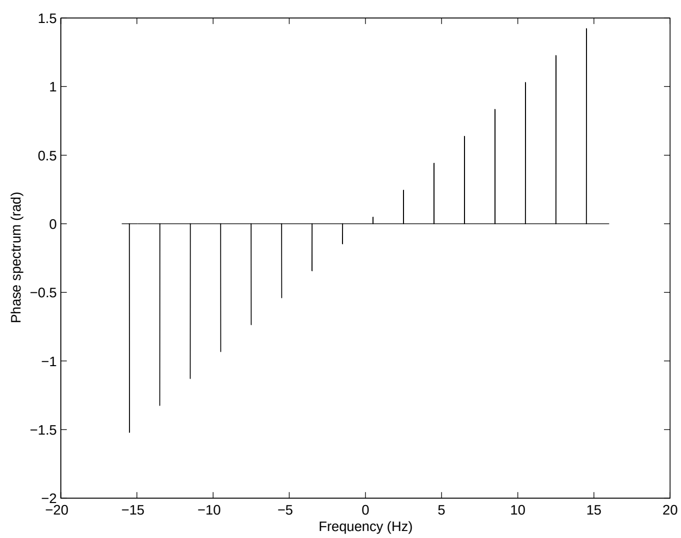

Figure 2

The phase difference spectrum

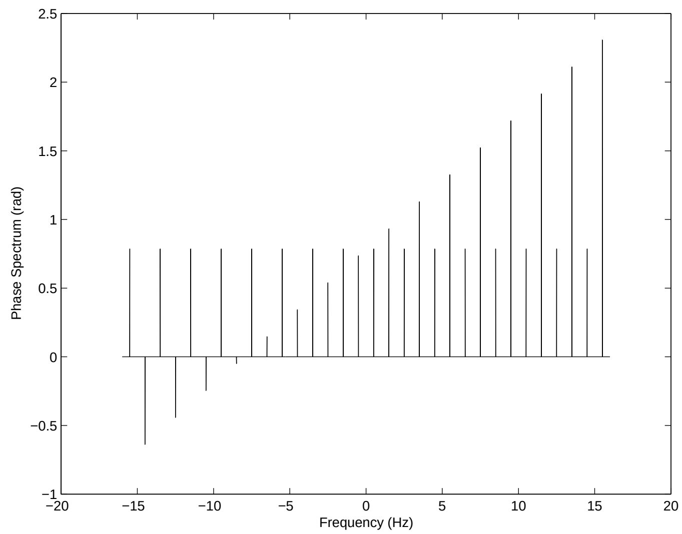

Figure 3

Problem 7.30

(a) Running the Matlab script provided in Appendix 7, the plots shown in Fig. 1 are obtained. The top plot of the figure shows the time-domain version of the bandpass signal. The carrier appears to show a small amount of amplitude modulation but this is due to the sampling process; if the sampling rate is increased by a factor of four, this amplitude modulation disappears as we would expect with rectangular pulse-shaping. The bottom plot of Fig. 1 shows the frequency-domain version of the bandpass signal. The plot is in the form of a (sin *x)/x* spectrum that is centered at the carrier frequency of 10 Hz, and the first null is offset by the bit rate of 1 Hz. The spectrum is not perfectly symmetric about the carrier due to aliasing, which affects the higher frequency components.

(b) We modify the provided Matlab script by inserting the statement
b = bIp + j*bQp;
and modifying the two statements
subplot(2,1,1), plot(t,real(b));   % time display
[spec,freq] = spectrum(b,nFFT,nFFT/4,nFFT/2,Fs);
With these changes, we obtain the plots shown in Fig. 2. The top plot of the figure shows the time-domain sequence of random data with rectangular pulse shaping. The bottom plot shows the (sin *x)/x* magnitude spectrum centered at the origin. In part (a), distortion of both the time-domain and frequency domain signals was noted due to the limitations of the sampling rate. In part (b), these distortions are much less evident. Consequently, if we simulate signals at complex baseband, then we may use much lower sampling rates (and thus less computational requirements) than for bandpass signals and obtain the same accuracy.

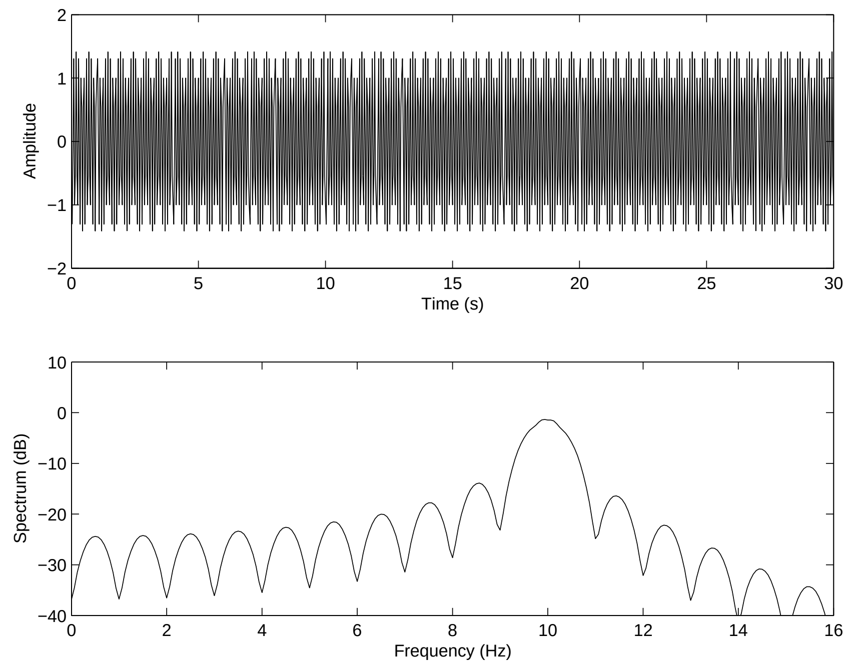

Figure 1

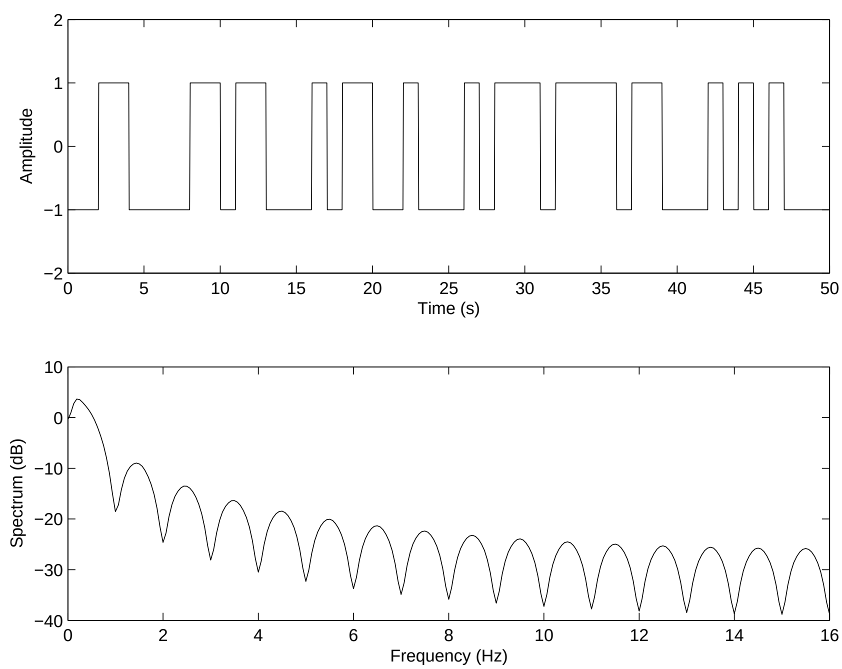

Figure 2

Problem 7.31

We modify the script of Problem 7.30(a) by replacing

```
Pulse Shape = ones(1,Fs); % rectangular pulse shape
```
With the lines
```
B0   = 0.5;                          % (Hz)
t    = [-2.001: 1/Fs : +2.001]       % time scale for pulse shape
rcos = sinc(4*B0*t) ./ (1-16*B0^2*t.^2);  % from Eq.(6.20)
Pulse Shape = rcos;
```

Doing so, we obtain the graphs plotted in Fig. 1. The top graph of the figure shows the time-domain version of the bandpass signal, including the amplitude modulation that occurs with raised cosine pulse-shaping. The bottom graph of the figure shows the raised cosine spectrum of the transmitted signal. Presence of the effects of aliasing is evident in the plot due to the spurious signal present at 0 Hz in the magnitude spectrum.

If we make changes similar to those of Problem 7.30(b), then we obtain the plots shown in Fig. 2. The top graph of the figure shows the baseband *I*-channel consisting of a random data stream with raised cosine pulse shaping. The bottom graph of the figure shows the magnitude spectrum of the complex baseband signal. There is no evidence of significant aliasing effects in this figure. The effects of aliasing are less evident in the raised-cosine case, because the spectrum is much more constrained than it is with rectangular pulse-shaping.

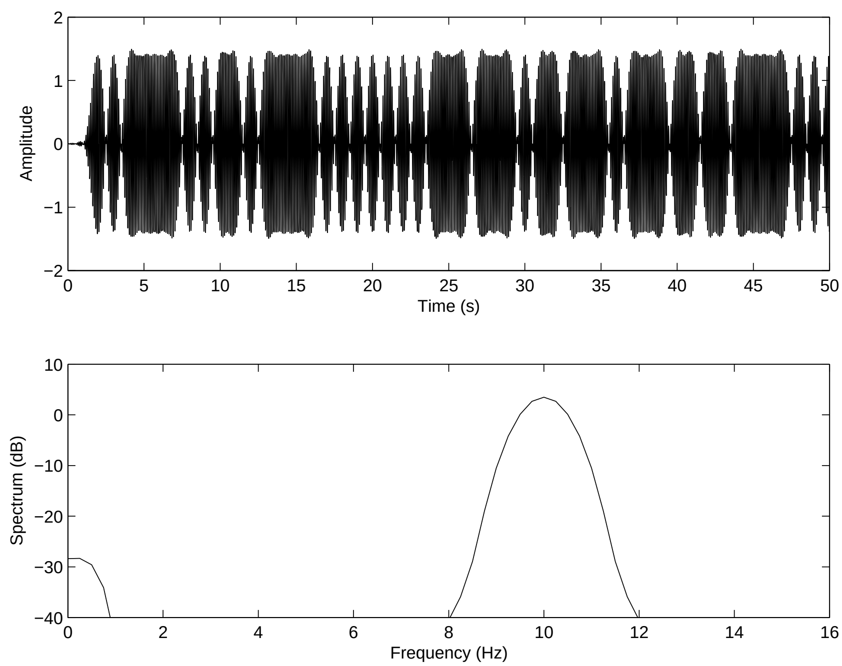

Figure 1

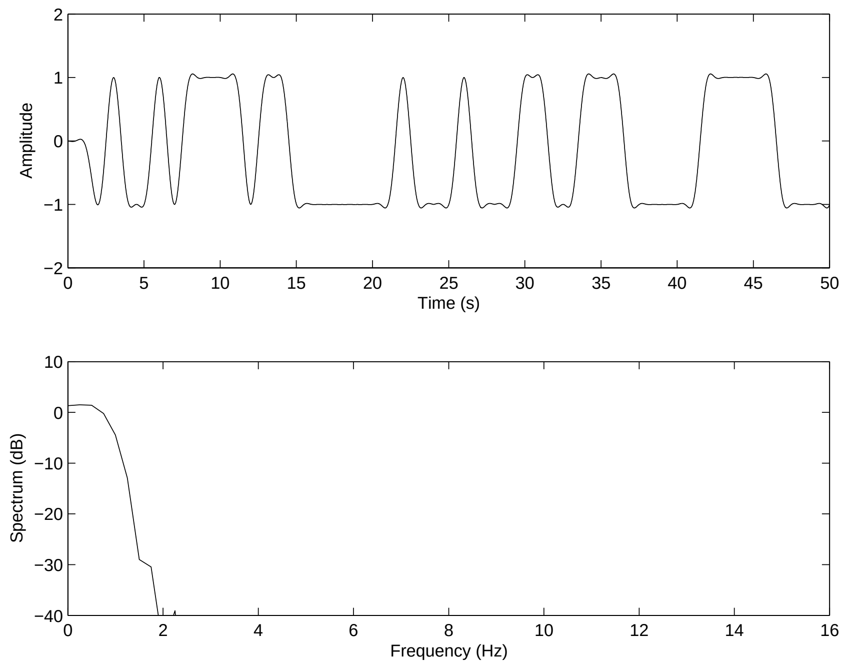

Figure 2